

Inferring untrained complex dynamics of delay systems using an adapted echo state network

Mirko Goldmann,^{*} Claudio R. Mirasso, Ingo Fischer, and Miguel C. Soriano[†]
*Instituto de Física Interdisciplinar y Sistemas Complejos (IFISC, UIB-CSIC),
 Campus Universitat de les Illes Balears E-07122, Palma de Mallorca, Spain*
 (Dated: November 9, 2021)

Caused by finite signal propagation velocities, many complex systems feature time delays that may induce high-dimensional chaotic behavior and make forecasting intricate. Here, we propose an echo state network adaptable to the physics of systems with arbitrary delays. After training the network to forecast a system with a unique and sufficiently long delay, it already learned to predict the system dynamics for all other delays. A simple adaptation of the network's topology allows us to infer untrained features such as high-dimensional chaotic attractors, bifurcations, and even multistabilities, that emerge with shorter and longer delays. Thus, the fusion of physical knowledge of the delay system and data-driven machine learning yields a model with high generalization capabilities and unprecedented prediction accuracy.

Due to many interacting entities with potentially multiple time scales, the prediction and analysis of complex systems represent a challenging task. Promoted by the increasing amount of available data, data-driven models such as deep learning have proven successful in numerous applications[1]. However, the use of machine learning solely trained on data can lead to unreasonable and nonphysical predictions[2]. Recently, a new method has emerged that fuses prior knowledge about certain characteristics of the system under study and trainable data-driven models. In so-called physics-informed machine learning, the design and training of the predictive model, e.g., a neural network, is biased by known physical models describing the character of the predicted system. This approach allows improving reliability and precision[3, 4]. A particularly challenging task is to predict the future of high-dimensional complex systems that exhibit chaotic behavior. Reservoir computing (RC) exhibits powerful capabilities in such tasks and offers fast training based on an analytically solvable linear regression[5]. The architecture of RC comprises three layers: a fixed input layer, a reservoir, and the trainable output layer. The input layer drives the processing unit called the reservoir that can be an echo state network. By weighting the reservoir states, the output layer computes the prediction[6–8]. Standard echo state networks efficiently predict chaotic time series of ordinary systems with high accuracy[9–15]. Furthermore, hybrid models based on the combination of model-free reservoir computing with a mathematical model of the task already showed improved performance in chaotic time series prediction.[16] However, many real-world systems feature a delay τ that makes them mathematically infinite-dimensional as they rely on a history function $h(t), t \in [0, -\tau]$ [17]. This can give rise to instabilities and cause a variety of complex phenomena including high-dimensional chaotic dynamics[18–21]. Due to that, chaotic time series generated by delay systems are widely used to benchmark the capabilities of predictive models[9, 14, 22–28]. However, as the complexity and di-

mensionality of such delay systems further increase with longer delays[19] many models with short-term memory, such as standard echo state networks, fail to handle the long-delayed time scale.

In this letter, we demonstrate the prediction of the high-dimensional dynamics of delay systems with arbitrary long delays. To this end, we encode prior knowledge about the model characteristics underlying the predicted time series directly into the topology of the reservoir. Then, we train this physics-informed network on a unique delay system using the reservoir computing paradigm. In the testing phase, we decouple the reservoir from the external input and it continues driven by its own prediction. If the reservoir is well-trained, it will replicate the dynamics of the system learned during training[14, 29]. In a second step, we adapt the reservoir's topology and the system infers dynamics of the learned system for delays not shown during the training. The reservoir can predict the entire bifurcation diagram of the delay system for arbitrary long delays. The proposed method enables data-efficient learning, high prediction accuracy, and generalization ability, which allows for predictions that reflect the physics of the learned dynamical system.

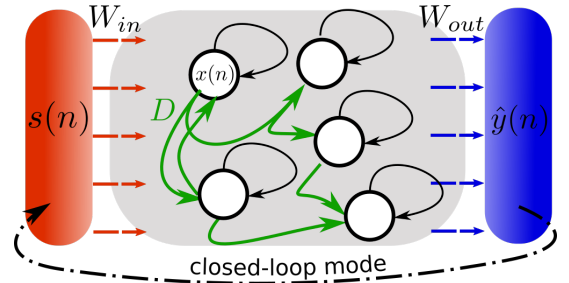


FIG. 1. Scheme of the delayed echo state network. The reservoir contains delayed internode weighted connections (green), where the delay D of the nodes connections can be adjusted.

In the following, we briefly introduce the delayed echo state network (dESN) illustrated in Fig. 1. The dESN

provides two independently tunable time scales linked to the delayed internode connections and a linear leak term. Hereby, all K nodes in the reservoir are delay coupled and evolve in a high dimensional phase space. This property makes the dESN well suited to adapt to the dynamics of a delay system. The dynamical evolution of the network is governed by:

$$\vec{x}(n+1) = \alpha \vec{x}(n) + \beta \tanh(\mathbf{W} \vec{x}(n-D) + \gamma \mathbf{W}_{in} s(n) + \mathbf{W}_b) \quad (1)$$

where $\vec{x}(n) \in \mathbb{R}^K$ are the reservoir states, α is the leak term, β is a feedback gain, γ is the input gain and D is the length of the delay. The delayed connection weights are given by $\mathbf{W} \in \mathbb{R}^{K \times K}$, which are randomly drawn from a uniform distribution $\mathcal{U}[-1, 1]$ and have a sparsity of 1.5%. The matrix $\mathbf{W}_{in} \in \mathbb{R}^{S \times K}$ gives the connection between the input $s(n) \in \mathbb{R}^S$ and the network while $\mathbf{W}_b \in \mathbb{R}^K$ gives a random bias to each node. For more details about the implementation of the dESN, we refer to the supplemental material[30]. During the training, the input $s(n)$ drives the reservoir and the output weights $\mathbf{W}_{out} \in K$ are computed to perform a one-step-ahead prediction $y(n) = s(n+1)$. Once the training is completed, the reservoir is decoupled from the input $s(n)$ and the prediction of the reservoir $\hat{y}(n) = \mathbf{W}_{out} \vec{x}(n)$ is fed back as the new input. Accordingly, the reservoir evolves autonomously in closed-loop mode.

To demonstrate the capabilities of the dESN, we consider forecasting a chaotic Mackey-Glass system[31] with a long delay as the task:

$$\dot{s}(t) = -0.1s(t) + \frac{0.2s(t-\tau)}{1 + s(t-\tau)^{10}}. \quad (2)$$

The delay of the system is set to $\tau = 100$ and $s(t)$ is sampled with $\Delta t = 1$. For these parameters, the system evolves along a chaotic attractor that has a Kaplan-Yorke dimension of $D_{KY} = 10.4$ [30]. Furthermore, $\tau = 100$ places the system in the long delay limit where the delay is much longer than the linear decay of the instantaneous dynamics in Eq. 2 (here 0.1^{-1}). Before training the dESN containing $K = 1000$ nodes, we match the delays of the reservoir's connections to the delay of the Mackey-Glass system by setting $D = \tau/\Delta t = 100$. We find that this matching improves the general prediction capabilities of the reservoir. All other hyperparameters are optimized using Bayesian optimization as given in [30]. The loss function is given by the absolute difference between the autonomously predicted and the Mackey-Glass time series initialized with the same initial conditions.

In Fig. 2, we show the prediction of the Mackey-Glass system with $\tau = 100$ by the dESN with $D = 100$. We divide the prediction capabilities into two regimes, which we term weather and climate. The weather refers to the short-term behavior after decoupling the input and the reservoir. As shown in Fig.2 a), the dESN can precisely

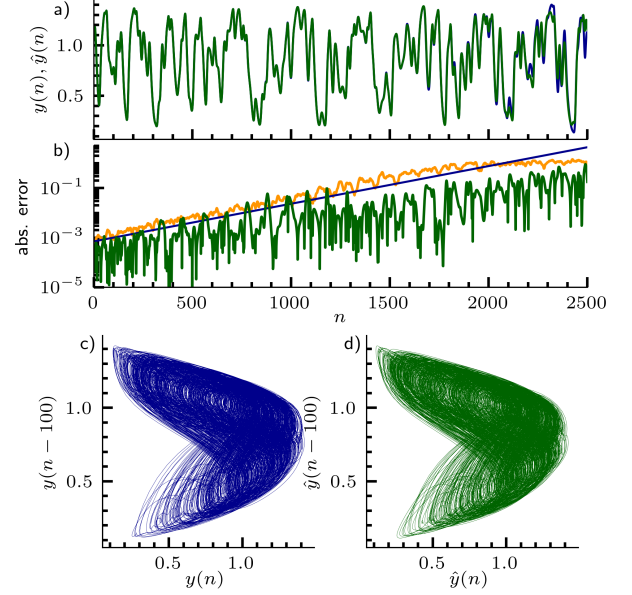


FIG. 2. a) Comparison of the time series of the original (blue) and the autonomously continued (green) chaotic attractor using a dESN. b) Divergence rate of the chaotic system and the time series generated by the dESN (green) as shown in a), the orange line indicates the average divergence rate of 20 different dESNs initialized at 20 different trajectories of the chaotic Mackey-Glass attractor. The blue line indicates the divergence rate related to the largest Lyapunov exponent $\lambda = 0.0035$ of the Mackey-Glass system with $\tau = 100$. In c) and d) we show the two dimensional representation of the chaotic attractor of the Mackey-Glass system with a delay of $\tau = 100$ and the dESN prediction with $D = 100$, respectively.

continue the trajectory for around 2000 steps, which corresponds to approximately seven Lyapunov times. The dESN learns the chaotic character of the Mackey-Glass system and both trajectories evolve together until they start to diverge. The divergence rate of the predicted trajectory is similar to the largest Lyapunov exponent of the Mackey-Glass system as depicted in Fig.2 b). Furthermore, the dESN prediction provides robustness against randomization, as we find similar results for 20 different dESNs with varied connection matrices and training data. The climate describes the long-term behavior of a dynamic system, e.g., the evolution along the chaotic attractor. In Fig.2 d), we show the predicted trajectory after it has diverged from the one it was initialized with. The dESN reproduces the climate of the delay system by predicting the chaotic attractor of the Mackey-Glass system with $\tau = 100$ as shown in Fig.2 c). Using the dESN, we can generate high-quality weather and climate predictions in the long delay regime.

We have checked that the dESN also provides high prediction accuracy for the Mackey-Glass system subjected to other delay times, e.g., $\tau = 17$ and $\tau = 30$, which are the delays usually employed in the literature

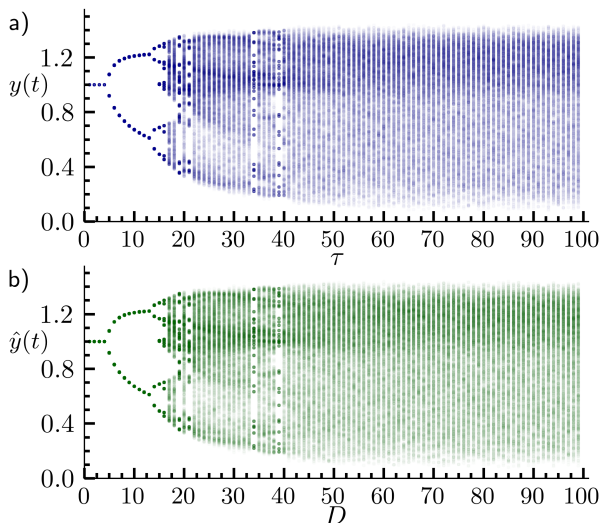


FIG. 3. a) Bifurcation diagram generated using the Mackey-Glass delay system. b) Bifurcation diagram predicted by scanning the D of a dESN trained on data of a Mackey-Glass system with $\tau = 100$.

for benchmark time series prediction. Compared to the results reported in [9] using standard echo state networks, we find that the dESN provides a higher accuracy for both tasks with $\log_{10}\text{NRMSE}_{84} = -6.18$ for $\tau = 17$ ($\log_{10}\text{NRMSE}_{84} = -5.09$ in [9]) and $\log_{10}\text{NRMSE}_{120} = -3.1$ for $\tau = 30$ ($\log_{10}\text{NRMSE}_{120} = -1.43$ in [9]) in the closed-loop mode. The higher prediction accuracy could further improve the controlling methods of such high-dimensional chaotic systems[28, 32, 33]. It is important to mention that there is no need to calibrate again the hyperparameters of the dESN using the Bayesian optimization, only the delay D needs to be adapted. The hyperparameters found for the prediction of the Mackey-Glass system with $\tau = 100$ yield high performance for any other delay.

In the following, we reveal the unprecedented generalization ability of our method by predicting for arbitrarily long delays while the dESN is trained solely on a Mackey-Glass system with $\tau = 100$. We let the reservoir evolve in the closed-loop mode, and without any retraining of the output weights, we vary the delay D of the node connections. The dynamics of the network nodes adapt after a short transient phase and the output of the dESN with modified D exhibits changes in its dynamical behavior. The bifurcation diagram shown in Fig. 3 illustrates that, depending on D , the dESN exhibits chaotic behavior, transitions to intermittent limit cycles, e.g., at $D = 34$ & 39 , period-doubling bifurcations at $D = 14$ & 16 , and the transition to a stable fixed point at $D = 5$. The observed transitions in the dESN coincide with those observed in the Mackey-Glass system, and the evolution of the chaotic attractor reveals sim-

ilar characteristics. In Fig. 4, we present a comparison of the two-dimensional representations of the attractors for several delays up to $\tau = 1000$ for the original and $D = 1000$ for the predicted system. We find that the dESN reproduces the attractors for all the shown examples even though it was solely trained with the time series of $\tau = 100$. Furthermore, the proposed dESN does not require an increase in the number of nodes if the delay length of the target increases. There is only a linear increase of required memory related to increasing delay as all states up to the delay D have to be stored. This demand can be compensated by using a single node with delay feedback relying on the delay-based reservoir approach[24, 34, 35]. In [30], we provide simulations that show that an optoelectronic reservoir exhibits similar capabilities in predicting long delay systems.

To further verify the climate prediction for different D , we compute the absolute difference Δ_{ACF} between the autocorrelation of the original and predicted attractor. In Fig. 5, we compare the prediction abilities of three different dESNs trained either on the data of a Mackey-Glass system with delay τ , $D = 17, 30$ or 100 . If a dESN is trained on the data of a short delay system, e.g., Mackey-Glass system with $\tau = 17$ or $\tau = 30$, it can predict the dynamics of respectively shorter delays. Nevertheless, deviations can appear and the predictions can fail as the predicted dynamics have higher dimension or higher complexity due to a delay D that is larger than the one used in the training. We observe that the dESNs trained with the Mackey-Glass system for $\tau = 17$ and $\tau = 30$ exhibit larger deviations and the predictions with longer delay D start to fail. In contrast, we demonstrate that by training the dESN with a longer delay, i.e., $\tau, D = 100$, we can successfully predict the dynamics related to shorter delays by decreasing the delay D of the dESN. Furthermore, by increasing the delay D , the prediction of systems with arbitrarily long delays becomes possible. The deviations in Δ_{ACF} in the range $\tau = 75 - 80$ observed for the ESN trained with $\tau, D = 100$ are related to the coexistence of a chaotic attractor and a limit cycle for the Mackey-Glass system. We show in [30] that depending on the initial conditions, the dESN converges to either one or the other. Röhmer et al.[13] recently presented that RC is capable of predicting multistabilities in a dynamical system even if the reservoir is trained only around a single attractor. Our trained dESN can predict multistabilities even if it is trained on an attractor that refers to a different parametrization of the original dynamical system.

Accordingly, the information carried in the training data sets plays an important role for the generalization ability of the dESN. To quantify this effect, we determine the complexity of an attractor using the Kolmogorov-Sinai entropy h_{KS} . Using the Pesin identity, the entropy h_{KS} is given by the sum of all positive Lyapunov exponents and defines the predictability of a chaotic system[36]. In the Mackey-Glass delay system, the number of positive

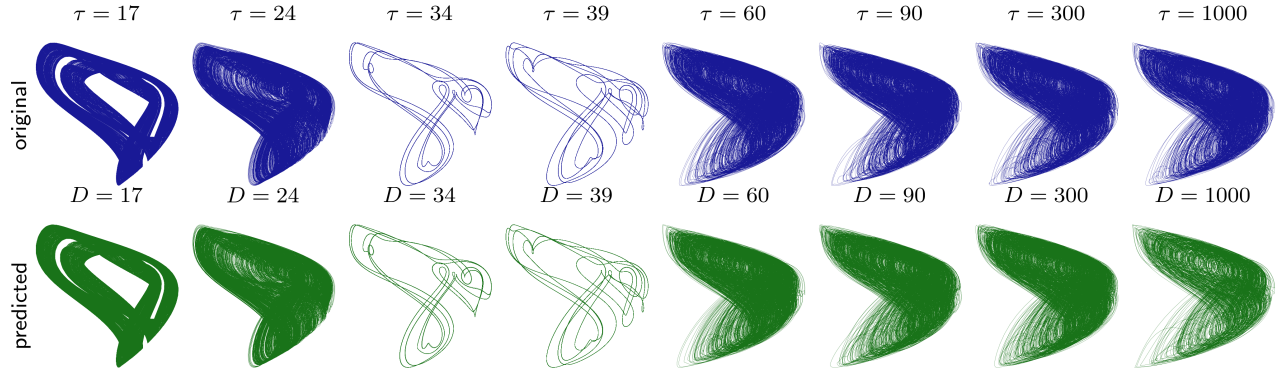


FIG. 4. Comparison of the attractor of the chaotic Mackey-Glass system and the prediction of these attractors generated using a dESN trained on a single local example of the Mackey-Glass system with $\tau = 100$. To generate the predicted attractors only the delay D of the dESN is changed. In this representation, the x-axis is the current state $y(t)$ and the y-axis is the delayed state $y(t - \tau)$.

Lyapunov exponents increases for longer delays. Nevertheless, their amounts shrink, and accordingly, the entropy and unpredictability of the system saturate in the limit of long delays [30, 37, 38]. We observe that training in the range of long delays [30, 37, 38]. We observe that training in the range of long delays, where the Kolmogorov-Sinai entropy saturates, e.g., $\tau = 100$, enables the dESN to predict precisely long and short delay dynamics. Using instead data in the training that originates from a delay below the long delay limit, e.g., $\tau = 30$, increases the probability of prediction failure for the emulation of Mackey-Glass dynamics with longer delays. The origin of this failure can be traced back to the inability to discriminate between the delay and the instantaneous dynamics of the Mackey-Glass system. We find that using training data from the delay in the range of the saturated entropy h_{KS} and a clear time-scale separation between the instantaneous and delay dynamics yields read-out weights of the dESN that allow the prediction of both short and long delay dynamics.

In general, by exploiting the prior knowledge about the physical model of the to-be-learned system, we design a neural network that predicts the complex dynamical evolution of high-dimensional systems with long delays using the RC scheme. Adapting the reservoir's topology after the training allows us to infer the entire bifurcation diagram of the learned delay system. Recently, an RC-based approach facilitated the prediction of transitions between different regimes of a dynamical system [39–41]. In those works, a time-dependent control parameter is fed to the reservoir simultaneously with the time series of the controlled system. After training the reservoir on multiple local examples, it evolves in the closed-loop mode and dynamical transitions that are not part of the training can be inferred by manipulating the control parameter. However, our method only requires a single local example, e.g., at $\tau = 100$, to precisely predict unseen dynamics notably distinct from that local example. Thereby,

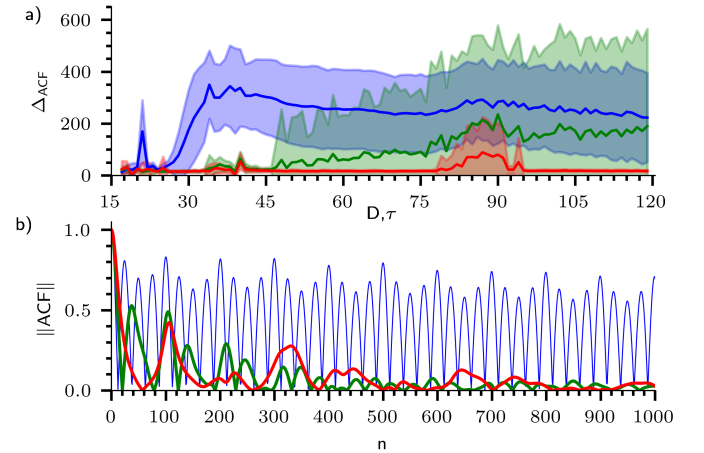


FIG. 5. Absolute difference of the original and the predicted autocorrelation Δ_{ACF} of the chaotic attractors a) in the range $\tau, D \in [17, 120]$. The colors refer to different delays of the Mackey-Glass system used in the training of the dESN, $\tau = 17$ (blue), $\tau = 30$ (green) and $\tau = 100$ (red). Solid lines indicate the average over 100 random seeds used to generate the dESN and initialize the Mackey-Glass system that generated the training data. The shaded areas indicate the standard deviation, respectively. b) Autocorrelation function of the Mackey-Glass system for different delays $\tau = 17, 30, 100$.

the adaptable topology of the network reduces the demands on the training data, and its predictions reflect the true physics of the learned system. Accordingly, our physics-informed reservoir provides a high ability to generalize. Furthermore, we note that the proposed mechanism works for other delay systems, e.g., the Ikeda-systems [30]. We argue that our approach has further potential for boosting the performance of other machine learning methods where the physical properties of the to-be-learned system are known a priori.

ACKNOWLEDGEMENTS

We acknowledge the Spanish State Research Agency, through the Severo Ochoa and María de Maeztu Program for Centers and Units of Excellence in R&D (MDM-2017-0711) and through the QUARESC project (PID2019-109094GB-C21 and -C22/ AEI / 10.13039/501100011033) and DECAPH project (PID2019-111537GB-C21 and -C22/ AEI / 10.13039/501100011033). M.G. acknowledges financial support by the European Union's Horizon 2020 research and innovation program under the Marie Skłodowska-Curie grant agreement No. 860360 (POST DIGITAL). The work of MCS has been supported by MICINN/AEI/FEDER and the University of the Balearic Islands through a "Ramon y Cajal" Fellowship (RYC-2015-18140). This work has been partially funded by the European Union's Horizon 2020 research and innovation programme under grant agreement No. 899265 (ADOPD).

* mirko@ifisc.uib-csic.es

† miguel@ifisc.uib-csic.es

- [1] Y. Tang, J. Kurths, W. Lin, E. Ott, and L. Kocarev, Introduction to focus issue: When machine learning meets complex systems: Networks, chaos, and nonlinear dynamics, *Chaos* **30**, 063151 (2020).
- [2] D. Lazer, R. Kennedy, G. King, and A. Vespignani, The parable of google flu: traps in big data analysis, *Science* **343**, 1203 (2014).
- [3] G. E. Karniadakis, I. G. Kevrekidis, L. Lu, P. Perdikaris, S. Wang, and L. Yang, Physics-informed machine learning, *Nat. Rev. Phys.* **3**, 422 (2021).
- [4] H. A. Elmarakeby, J. Hwang, R. Arafeh, J. Crowdis, S. Gang, D. Liu, S. H. AlDubayan, K. Salari, S. Kregel, C. Richter, *et al.*, Biologically informed deep neural network for prostate cancer discovery, *Nature* **598**, 348–352 (2021).
- [5] M. Lukoševičius, H. Jaeger, and B. Schrauwen, Reservoir computing trends, *KI-Künstliche Intelligenz* **26**, 365 (2012).
- [6] H. Jaeger, The "echo state" approach to analysing and training recurrent neural networks-with an erratum note, Bonn, Germany: German National Research Center for Information Technology GMD Technical Report **148**, 13 (2001).
- [7] W. Maass, T. Natschläger, and H. Markram, Real-time computing without stable states: A new framework for neural computation based on perturbations, *Neural Comput.* **14**, 2531 (2002).
- [8] K. Nakajima and I. Fischer, eds., *Reservoir Computing: Theory, Physical Implementations, and Applications*, Natural Computing Series (Springer, Singapore, 2021).
- [9] H. Jaeger and H. Haas, Harnessing Nonlinearity: Predicting Chaotic Systems and Saving Energy in Wireless Communication, *Science* **304**, 78 (2004).
- [10] J. Pathak, Z. Lu, B. R. Hunt, M. Girvan, and E. Ott, Using machine learning to replicate chaotic attractors and calculate lyapunov exponents from data, *Chaos* **27**, 121102 (2017).
- [11] J. Pathak, B. Hunt, M. Girvan, Z. Lu, and E. Ott, Model-free prediction of large spatiotemporally chaotic systems from data: A reservoir computing approach, *Phys. Rev. Lett.* **120**, 024102 (2018).
- [12] C. Klos, Y. F. K. Kossio, S. Goedeke, A. Gilra, and R.-M. Memmesheimer, Dynamical learning of dynamics, *Phys. Rev. Lett.* **125**, 088103 (2020).
- [13] A. Röhm, D. J. Gauthier, and I. Fischer, Model-free inference of unseen attractors: Reconstructing phase space features from a single noisy trajectory using reservoir computing, *Chaos* **31**, 103127 (2021).
- [14] P. Antonik, M. Gulina, J. Pauwels, and S. Massar, Using a reservoir computer to learn chaotic attractors, with applications to chaos synchronization and cryptography, *Phys. Rev. E* **98**, 1 (2018), 1802.02844.
- [15] Z. Lu, B. R. Hunt, and E. Ott, Attractor reconstruction by machine learning, *Chaos* **28**, 061104 (2018).
- [16] J. Pathak, A. Wikner, R. Fussell, S. Chandra, B. R. Hunt, M. Girvan, and E. Ott, Hybrid forecasting of chaotic processes: Using machine learning in conjunction with a knowledge-based model, *Chaos* **28**, 041101 (2018).
- [17] T. Erneux, *Applied delay differential equations*, Vol. 3 (Springer Science & Business Media, 2009).
- [18] I. Fischer, O. Hess, W. Elsässer, and E. Göbel, High-dimensional chaotic dynamics of an external cavity semiconductor laser, *Phys. Rev. Lett.* **73**, 2188 (1994).
- [19] M. Le Berre, E. Ressayre, A. Tallet, and H. M. Gibbs, High-dimension chaotic attractors of a nonlinear ring cavity, *Phys. Rev. Lett.* **56**, 274 (1986).
- [20] S. Heiligenthal, T. Dahms, S. Yanchuk, T. Jüngling, V. Flunkert, I. Kanter, E. Schöll, and W. Kinzel, Strong and weak chaos in nonlinear networks with time-delayed couplings, *Phys. Rev. Lett.* **107**, 234102 (2011).
- [21] G. C. Sethia, A. Sen, and F. M. Atay, Clustered chimera states in delay-coupled oscillator systems, *Phys. Rev. Lett.* **100**, 144102 (2008).
- [22] R. Hegger, M. J. Bünner, H. Kantz, and A. Giaquinta, Identifying and modeling delay feedback systems, *Phys. Rev. Lett.* **81**, 558 (1998).
- [23] B. Penkovsky, X. Porte, M. Jacquot, L. Larger, and D. Brunner, Coupled nonlinear delay systems as deep convolutional neural networks, *Phys. Rev. Lett.* **123**, 054101 (2019).
- [24] P. Antonik, M. Haelterman, and S. Massar, Brain-inspired photonic signal processor for generating periodic patterns and emulating chaotic systems, *Phys. Rev. Appl.* **7**, 054014 (2017).
- [25] M. Goldmann, F. Köster, K. Lüdge, and S. Yanchuk, Deep time-delay reservoir computing: Dynamics and memory capacity, *Chaos* **30**, 093124 (2020).
- [26] X. Chen, T. Weng, H. Yang, C. Gu, J. Zhang, and M. Small, Mapping topological characteristics of dynamical systems into neural networks: A reservoir computing approach, *Phys. Rev. E* **102**, 033314 (2020).
- [27] B. A. Marquez, J. Suarez-Vargas, and B. J. Shastri, Takens-inspired neuromorphic processor: A downsizing tool for random recurrent neural networks via feature extraction, *arXiv* **1**, 33030 (2019), 1907.03122.

- [28] Q. Zhu, H. Ma, and W. Lin, Detecting unstable periodic orbits based only on time series: When adaptive delayed feedback control meets reservoir computing, *Chaos* **29**, 093125 (2019).
- [29] A. Haluszczyński and C. R  th, Good and bad predictions: Assessing and improving the replication of chaotic attractors by means of reservoir computing, *Chaos* **29**, 10.1063/1.5118725 (2019), 1907.05639.
- [30] See Supplemental Material at [URL will be inserted by publisher] for the results of the dESN performing the closed-loop mode continuation of the Mackey-Glass system with $\tau = 17$ and $\tau = 30$, respectively. Further, we explain how to implement a delay-based reservoir such that it has similar capabilities as the dESN. Finally, we show the results of training a dESN to predict the bifurcation diagram of an Ikeda delay system.[42, 43].
- [31] M. C. Mackey and L. Glass, Oscillation and chaos in physiological control systems, *Science* **197**, 287 (1977).
- [32] W.-X. Wang, Y.-C. Lai, and C. Grebogi, Data based identification and prediction of nonlinear and complex dynamical systems, *Phys. Rep.* **644**, 1 (2016).
- [33] H. Ma, W. Lin, and Y.-C. Lai, Detecting unstable periodic orbits in high-dimensional chaotic systems from time series: Reconstruction meeting with adaptation, *Phys. Rev. E* **87**, 050901 (2013).
- [34] L. Appeltant, M. C. Soriano, G. Van Der Sande, J. Danckaert, S. Massar, J. Dambre, B. Schrauwen, C. R. Mirasso, and I. Fischer, Information processing using a single dynamical node as complex system, *Nat. Commun.* **2**, 466 (2011).
- [35] F. K  ster, D. Ehlert, and K. L  dge, Limitations of the recall capabilities in delay-based reservoir computing systems, *Cognit Comput* , 1 (2020).
- [36] J. Pesin, Characteristic lyapunov exponents and smooth ergodic theory, *Russ. Math Surveys* **32**, 55 (1977).
- [37] R. Vicente, J. Daud  n, P. Colet, and R. Toral, Analysis and characterization of the hyperchaos generated by a semiconductor laser subject to a delayed feedback loop, *IEEE J. Quantum Electron.* **41**, 541 (2005).
- [38] J. D. Farmer, Chaotic attractors of an infinite-dimensional dynamical system, *Physica D* **4**, 366 (1982).
- [39] J. Z. Kim, Z. Lu, E. Nozari, G. J. Pappas, and D. S. Bassett, Teaching recurrent neural networks to infer global temporal structure from local examples, *Nat. Mach. Intell.* **3**, 316 (2021).
- [40] L.-W. Kong, H. Fan, C. Grebogi, and Y.-C. Lai, Emergence of transient chaos and intermittency in machine learning, *JPhys Complexity* **2**, 035014 (2021).
- [41] L.-W. Kong, H.-W. Fan, C. Grebogi, and Y.-C. Lai, Machine learning prediction of critical transition and system collapse, *Phys. Rev. Res.* **3**, 13090 (2021), 2012.01545.
- [42] L. Larger, B. Penkovsky, and Y. Maistrenko, Virtual chimera states for delayed-feedback systems, *Phys. Rev. Lett.* **111**, 054103 (2013).
- [43] T. Erneux, L. Larger, M. W. Lee, and J.-P. Goedgebuer, Ikeda hopf bifurcation revisited, *Physica D* **194**, 49 (2004).